Catal Lett (2008) 124:139–145
DOI 10.1007/s10562-008-9441-5

Isomerization of Norbornadiene to Quadricyclane Using Ti-Containing MCM-41 as Photocatalysts

Ji-Jun Zou · Ming-Yue Zhang · Bin Zhu · Li Wang · Xiangwen Zhang · Zhentao Mi

Received: 21 November 2007 / Accepted: 11 February 2008 / Published online: 5 March 2008

Abstract Heterogeneous Ti-containing MCM-41 materials were prepared for the photocatalytic isomerization of norbornadiene to quadricyclane with the aim of replacing homogeneous sensitizers. Chemical grafting produces quantum-size TiO_2 crystallites highly dispersed in the pore of MCM-41. Isomorphous substitution generates Ti species in the framework of MCM-41, but some non-framework species are formed with increasing Ti content. It is found that Ti-containing MCM-41 materials show significantly higher photocatalytic activity than bulk TiO_2, and the framework Ti species are more active than the surface-dispersed species.

Keywords Photocatalyst · Ti–MCM-41 · Norbornadiene · Quadricyclane · Isomerization

1 Introduction

Photocatalytic valance isomerization of norbornadiene(NBD, bicyclo[2.2.1]hepta-2,5-diene) to quadricyclane(QC, tetracyclo[3.2.0.0^{2,7}.0^{4,6}]heptane) has been regarded as an effective way to store solar energy for decades [1–3]. In this reaction, about 89 kJ of energy is stored in one mole of QC molecules due to its highly-strained structure. The stored energy can be released through the inverse reaction under specific conditions. QC is a liquid with melting point of −40 °C, density of 0.98 g/mL (20 °C), and combustion heat of 44.9 MJ/kg [4]. It is stable under atmospheric conditions, thus can be easily stored, transported and handled. During combustion, the strained energy released can significantly increase the heat value. So QC has been considered as a potential high-energy density liquid fuel for the replacement or additives of current hydrocarbon fuels. It is reported that the H_2O_2/QC mixture shows higher specific impulse than the mixture based on RP-1 that is a widely used rocket fuel [4, 5]. It is also considered as a non-toxic high energy fuel in satellite control system to replace the highly toxic hydrazine [6].

The isomerization of NBD to QC occurs under irradiation, but the reaction has to be assisted with sensitizers or photocatalysts because the NBD molecules cannot absorb solar energy directly. The sensitizer-catalytic isomerization has been widely investigated. Many sensitizers like Michler's Ketones, benzenzophenone, $CuCl_2$ and Ru compounds have been used for this reaction [7–9]. Although these sensitizers show high activity and selectivity, they, unfortunately, suffer from some drawbacks. The sensitizers are not stable under irradiation and prone to decompose. Homogenous sensitizers are soluble in the reactant solution, which hinders the recycling of sensitizers and purification of product. From the point view of practical application, heterogeneous photocatalysts are more favorable. In a short technical note, it was reported that semiconductors including ZnO, ZnS and CdS could catalyze the isomerization of NBD [10], but no further details are reported after that. It also has been reported that NBD absorbed in the cages of cation-exchanged Y zeolites is isomerized to QC [11].

TiO_2 is a well-known and extensively investigated photocatalyst, which has been used in many photocatalytic processes such as degradation of organics, oxidation of

J.-J. Zou · M.-Y. Zhang · B. Zhu · L. Wang (✉) · X. Zhang · Z. Mi
Key Laboratory for Green Chemical Technology of Ministry of Education, School of Chemical Engineering and Technology, Tianjin University, Tianjin 300072, China
e-mail: wlytj@yahoo.com.cn

J.-J. Zou
e-mail: jj_zouchem@yahoo.com.cn

gaseous pollutants, and hydrogen generation from alcohols and water [12]. However, this semiconductor suffers from a relatively low photo-activity because of the low efficiency in optical absorption and charge separation. It has been found that TiO_2 species highly dispersed in the cavitites and framework of zeolites exhibit high photocatalytic reactivity [13–17]. MCM-41 has a well-defined array of uniform hexagonal mesopores with large internal surface area, exhibiting great potential applications as the supports of TiO_2. It has been reported that incorporation of Ti into MCM-41 framework gives unique photocatalytic activity [13–16]. In addition, it has been claimed that the photocatalytic activity of TiO_2 is increased when loaded on mesoporous silica support [14, 17].

The aim of present work is to use heterogeneous TiO_2, instead of homogenous sensitizers, as the photocatalyst for the QC synthesis reaction. To improve the activity, TiO_2 was dispersed on MCM-41 through chemical grafting and isomorphous substitution methods. The prepared materials were characterized and the activities were evaluated. A possible reaction mechanism was also suggested.

2 Experimental

2.1 Synthesis of Materials

MCM-41 was synthesized by hydrothermal method using tetrathyorthosilicate (TEOS) as the starting materials and cetyltrimethylammonium bromide (CTABr) as the structure directing agent [18–20]. At 40 °C, CTABr (1.82 g) was dissolved in aqueous solution (45 mL) containing NaOH (0.4 g). Then TEOS (8.21 mL) was added dropwise. The solution was stirred vigorously for 1 h to ensure the hydrolysis of TEOS. The resulting gel was transferred to a Teflon-lined autoclave and held at 100 °C for 3 days, and then it was filtered, washed with deionized water and anhydrous ethanol, and dried at 100 °C overnight. The materials thus obtained were calcined at 500 °C for 5 h with a temperature rising rate of 2 °C/min to produce white MCM-41 powders.

Ti-substituted materials were synthesized by isomorphous substitution. The procedure is similar to the synthesis of MCM-41 except that defined amount of tetrabutyl titanate (TBOT) was added dropwise into the hydrolysized gel of TEOS and stirred for another hour. Three samples with the Si/Ti molar ratio in the stating materials as 70, 50 and 30 were synthesized and referred to as Ti–MCM-41(70), Ti–MCM-41(50) and Ti–MCM-41(30), respectively. The actual Ti content of the final materials was measured using ICP and shown in Table 1.

TiO_2-dispersed materials were synthesized by chemical grafting. TBOT (5 mL) and as-prepared MCM-41 (1 g) were added in *n*-hexane (50 mL), refluxed at 70 °C for 24 h under N_2 atmosphere. TBOT was supposed to be grafted on MCM-41. Then it was filtered and washed with anhydrous ethanol to remove the TBOT residues. The TBOT grafted on MCM-41 was hydrolyzed by adding deionized water (10 mL) under stirring. After that the materials were filtered, washed, dried overnight, and calcined at 500 °C for 3 h with a temperature rising rate of 2 °C/min. The synthesized material was referred as TiO_2–MCM-41.

For reference, TiO_2 powders were prepared via sol–gel process. The sol obtained by hydrolysis with $NH_3 \cdot H_2O$ was aged at room temperature for 4 h, dried at 100 °C for 8 h and calcined at 500 °C for 3 h. XRD and physical adsorption characterizations determined that it is composed by 100% anatase with a specific surface area of 38.8 m^2/g.

2.2 Characterizations of Materials

XRD characterizations were conducted at room temperature using an X'Pert PRO X-ray diffractometer equipped with Co radiation at 40 kV and 30 mA. UV–Visible diffuse reflectance spectra were recorded using a Shimadzu UV-3600 spectrometer. FT-IR characterizations were conducted on a Magna-IR 560 infrared spectrometer. Prior to spectroscopic measurements, the materials were degassed at 500 °C for 1 h to exclude absorbed water. TEM observations were carried out using a Tecnai G2 F-20 transmission electron microscope. N_2 adsorption–desorption isotherms

Table 1 Physicochemical properties of as-prepared Ti-containing materials

Samples (*x*)	Ti content in final materials (wt.%)	d_{100} (nm)	a_0 values (nm)	SBET ($m^2\ g^{-1}$)	Pore volume ($cm^3\ g^{-1}$)	Pore size (nm)
MCM-41	–	3.65	4.21	1130.4	0.83	2.69
TiO_2–MCM-41	5.79	3.69	4.26	1095.2	0.74	2.68
Ti–MCM-41(70)	0.43	3.72	4.30	1163.2	0.89	3.02
Ti–MCM-41(50)	0.54	3.77	4.35	618.4	0.49	2.99
Ti–MCM-41(30)	0.79	3.78	4.39	375.9	0.20	2.66

were performed at 77 K with a Micromeritics Tristar 300 instrument. Samples were degassed at 100 °C for 5 h prior to the measurements. The actual Ti content in the final materials was determined by ICP using a Varian Vista-MPX instrument.

2.3 Photocatalytic Reaction

The photocatalytic isomerization of NBD to QC was illustrated as Scheme 1. This reaction was conducted in an inner irradiation quartz chamber with a volume of 250 mL. A 400 W high-pressure Hg lamp with outside water cooling jacket was placed in the center of reactor. NBD (10 mL) and photocatalyst powders (0.1 g) were suspended in dimethyl benzene (220 mL) by a magnetic stirrer. The reaction was carried out for 12 h at 25 °C, and a sample was withdrawn at regular intervals for analysis. The samples were analyzed using a HP 4890 chromatograph equipped with a BP-1capillary column (25 m × 0.33 mm × 0.05 μm), with N_2 as the carrier gas and FID as the detector.

3 Results and Discussion

3.1 XRD Patterns

Figure 1 is the XRD patterns of synthesized materials. MCM-41 shows a strong peak at $2\theta = 2$–$3°$ and two weak peaks at 4–5° corresponding to (100), (110), and (200) reflexes [20, 21], which are characteristic of ordered mesoporous materials with hexagonal structure. TiO_2–MCM-41 shows three identical diffraction peaks, indicating that grafting of TiO_2 in the pore of MCM-41does not influence the ordered hexagonal structure of supports. An additional peak corresponding to the (101) reflex of anatase TiO_2 is observed at 25.5°, but the intensity is extremely weak. This indicates that TiO_2 crystallites are highly dispersed in the pore of MCM-41.

Ti–MCM-41 shows XRD patterns with intensity and diffraction angle different from MCM-41 and TiO_2–MCM-41. The intensity of the characteristic d_{100} peak decreases, which is more obvious with increasing Ti content.

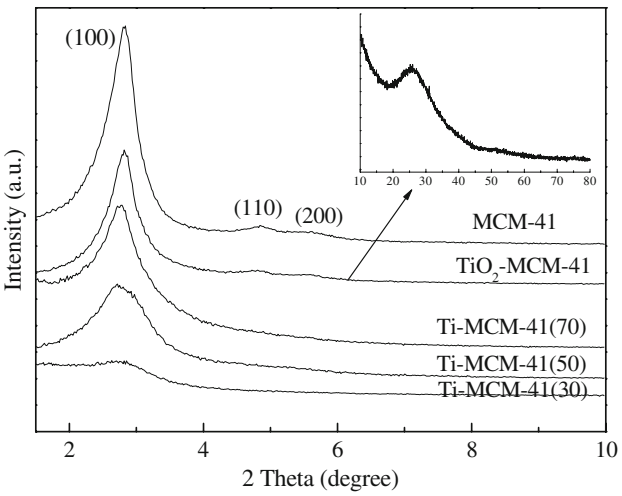

Fig. 1 XRD patterns of as-prepared Ti-containing materials

Moreover, the d_{110} and d_{200} peaks completely disappear. These results suggest that the structural integrity of MCM-41 is impaired due to the incorporation of Ti atoms. This phenomenon is specifically evident when the Si/Ti ratio is less than 50, because the ordered structure is greatly destroyed. At the same time, the (100) peak shifts to higher diffraction angle in XRD patterns. Table 1 also shows an obvious increase in the d spacing and a_0 values with increasing Ti content. Since the Ti–O bond distance is longer than the Si–O bond distance, it is reasonable that the incorporation of Ti ions in the framework enlarges the cell unit of the as-prepared materials. There is no evidence of TiO_2 crystallites formation, because no other peaks are observed in wide range XRD patterns. This indicates that Ti atoms either atomically disperse in the framework positions or exist in an amorphous dispersed form in the pore of MCM-41.

3.2 UV–Visible Diffuse Reflectance Spectra

UV–Vis diffuse reflectance spectra spectroscopy has been widely used to characterize the nature and coordination of Ti^{4+} ions in Ti-containing molecular sieves. Figure 2 shows the UV–Vis DRS of the samples prepared in this work. Pure MCM-41 shows no absorption in the region

Scheme 1 Photocatalytic isomerization of NBD to QC over Ti-containing MCM-41

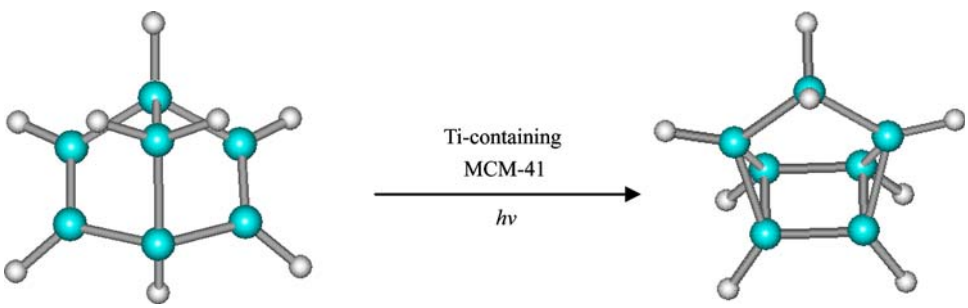

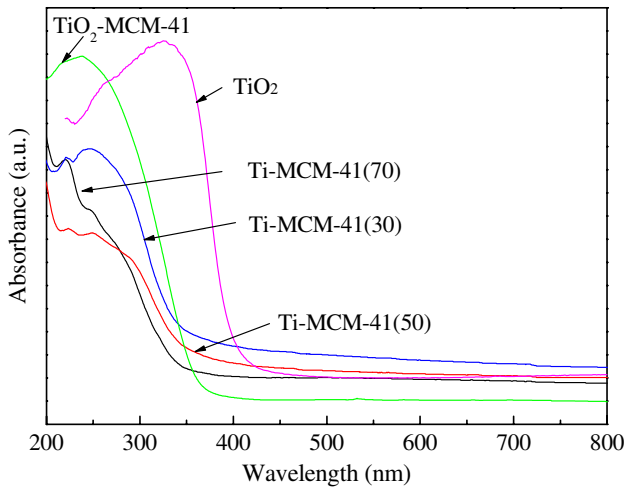

Fig. 2 UV–Vis diffuse reflectance spectra of as-prepared Ti-containing materials

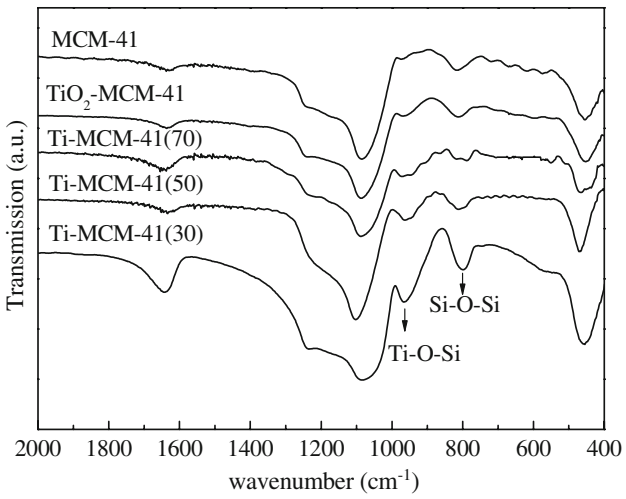

Fig. 3 FI-IR spectra of as-prepared Ti-containing materials

>200 nm because this absorption band is caused by Ti species. Ti–MCM-41(70) shows an absorption peak at 220 nm, which can be ascribed to the charge transfer from oxygen ligands to tetracoordinated Ti [17, 22, 23]. This is the direct evidence for the existence of isolated tetrahedral Ti (Ti–O–Si) in the framework of MCM-41. Besides the band at 220 nm, Ti–MCM-41(50) and Ti–MCM-41(30) have a shoulder peak at ~270 nm belonging to Ti species in higher coordination environments (penta- or hexacoordinatied species) [17, 22, 23], suggesting that some Ti ions exist as non-framework Ti and even polymerized species (Ti–O–Ti). It is clear that most of the Ti species are dispersed in the framework (Ti–O–Si) of Ti–MCM-41 when the Ti content is low, but polymerized Ti species (Ti–O–Ti) and even nanodomains of amorphous TiO_2–SiO_2 are present in the materials when the Ti content is high.

For TiO_2–MCM-41, a broad band at ~260 nm is observed, which is assigned to the Ti-oxide species [23]. This suggests that the grafted titanium mainly exists as oxide particles in the pore of matrix materials. Compared with bulk TiO_2, the absorption band is largely shifted to blue region, because these TiO_2 crystallites are highly dispersed in quantum-size.

3.3 FT-IR Spectra

Figure 3 is the IR spectra of the prepared materials. All of them show an absorption band at ~960 cm^{-1}, which has been interpreted in terms of the presence of Si–OH groups and Ti–O–Si bonds [16, 23]. As shown in Fig. 3, this band is rather weak in pure silica MCM-41. It slightly increases for TiO_2–MCM-41, suggesting that some Ti–O–Si bonds are formed by chemical grafting. However, the amount of these bonds is limited because the band is still very weak, which shows that most of the titanium species are dispersed on the pore surface of MCM-41 in form of crystallites. For Ti–MCM-41, the intensity of IR absorption band systematically increases with increasing Ti content. This tendency clearly shows that more Ti–O–Si bonds are formed, thus most of the Ti species are incorporated in the framework of MCM-41 through isomorphous substitution, in agreement with UV–Vis and XRD characterizations.

The incorporation of Ti into framework increases the asymmetry of MCM-41 structure and enhances the intensity of IR band at ~960 cm^{-1}. However, the band at ~800 cm^{-1} assigned to the symmetric vibration of Si–O–Si bonds should not be influenced by the substitution [16, 23]. So the intensity ratio of the band at 960 cm^{-1} to that at 800 cm^{-1} should increase with the incorporation of Ti in the framework of silica zeolites. TiO_2–MCM-41 shows a slight increase in the ratio compared with pure MCM-41, confirming that only a few Ti ions are incorporated in the framework. Meanwhile Ti–MCM-41materials have obviously higher ratio than MCM-41 and TiO_2–MCM-41. Moreover, the ratio continuously rises up with the increase of Ti content, testifying that more Ti ions are incorporated in the framework.

3.4 TEM Images

Figure 4 shows the TEM images of as-prepared materials. MCM-41 exhibits uniform and regular pore with size of 2 nm. TiO_2–MCM-41 also shows uniform pore structure, confirming that grafting TiO_2 does not influence the structure of parent materials. EDX analysis shows the atomic ratio of Si/Ti is 12, in agreement with the ICP analysis. However, no TiO_2 nanoparticles are observed inside the pore of MCM-41, confirming that TiO_2 crystallites are highly dispersed in crystallites. EDX analysis does

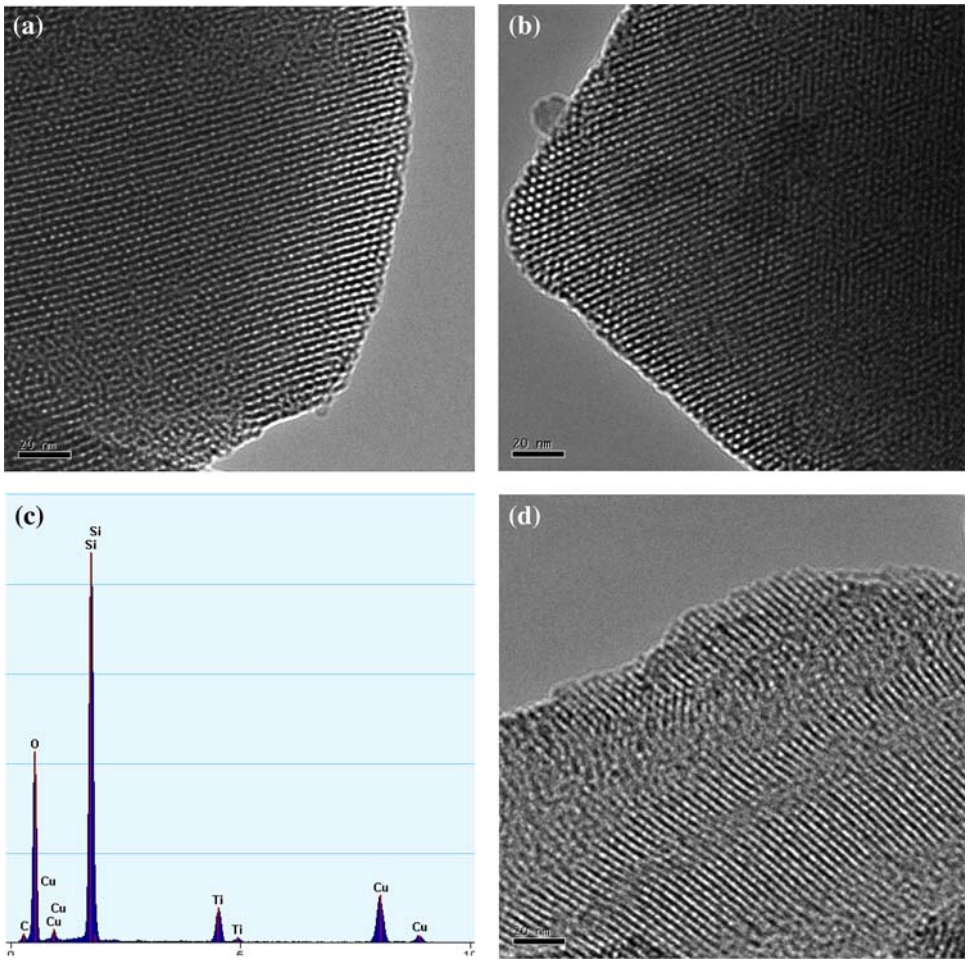

Fig. 4 TEM images of (**a**) MCM-41, (**b**) TiO_2–MCM-41 with (**c**) its EDX spectrum, and (**d**) Ti–MCM-41(50)

not detect any Ti element in Ti–MCM-41 because the Ti content in the materials is very low. However, significant change in morphology is observed. The materials no longer show uniform pore structure, and many linear tubular pores collapse into irregular pores. Moreover, some pores are blocked by amorphous fragments broken off from the wall. This clearly shows that incorporation of Ti in the framework greatly interrupt the Si–O–Si network and decrease the integrity of pore structure, in agreement with XRD characterizations.

3.5 N_2 Adsorption–Desorption

Figure 5 shows the N_2 adsorption–desorption isotherms of as-prepared materials. All of them show type IV classification, which is typical adsorption of mesoporous materials [17, 20]. MCM-41 and TiO_2–MCM-41 shows a steep increase in the adsorption isotherm in the P/P_0 range of 0.25–0.4, again confirming that grafting TiO_2 neither forms bulk particles nor influences the uniform pore structure of parent MCM-41. In the case of Ti–MCM-41 materials, the incorporation of Ti in the framework greatly destroys the pore structure, as has been shown by XRD and TEM. Therefore the adsorption–desorption isotherms become much flat with increasing Ti content. The textual parameters in Table 1 provide further evidences. TiO_2–MCM-41

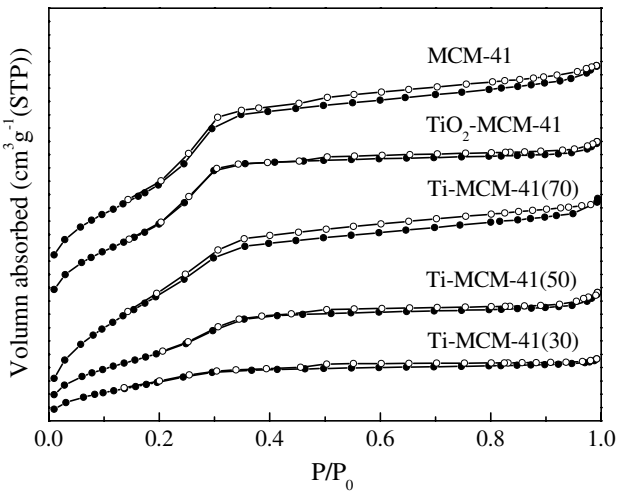

Fig. 5 N_2 absorption–desorption isotherms of as-prepared Ti-containing materials

and MCM-41 have similar surface area, pore volume and pore size. On the contrary, Ti–MCM-41 has continuously decreasing surface area, pore volume and pore size with the increase of Ti content. It is noticed that Ti–MCM-41(50) and Ti–MCM-41(30) shows a dramatic loss in specific surface area and pore volume. Two factors may account for this result. First, the incorporation of Ti in framework inhibits the formation of ordered pores. Second, many ordered pores collapse into irregular and even blocked pores during calcination.

3.6 Photocatalytic Activity

Figure 6 shows the photocatalytic performance of as-prepared materials. Since the isomerization of NBD to QC is highly selective (almost 100%), the yield of QC is used to evaluate the activity. It can be seen that bulk TiO_2 can catalyze the reaction, but the activity is very low because of its inherent defects such as low optical absorption and slow charge separation. TiO_2–MCM-41 shows a doubled yield of QC. This is attributed to the TiO_2 crystallites highly dispersed in the pore of MCM-41, which exhibit favorable quantum-size effect with high optical absorption and fast charge transfer rate. Incorporation Ti ions in the framework of MCMC-41 further improves the activity because the isolated tetrahedral Ti–O species is significantly active for photocatalytic reaction. As a result, Ti–MCM-41(30) shows a highest yield of 91.8% after 12 h. Ti–MCM-41(70) shows a relatively lower yield due to the very low Ti content.

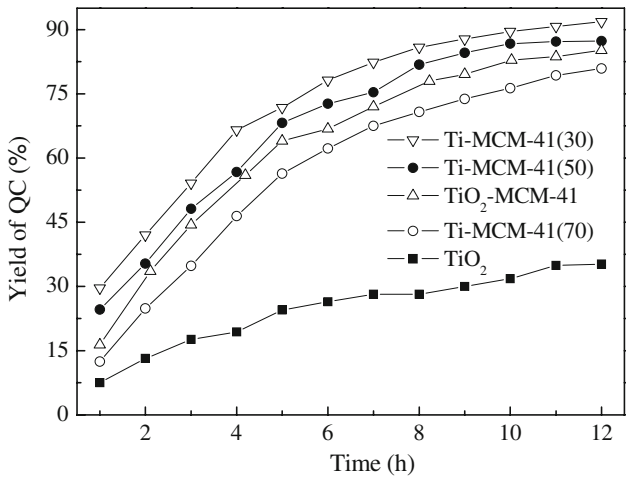

Fig. 6 Phtocatalytic activity of as-prepared Ti-containing materials. (Reactant mixture: 0.1 catalyst, 10 mL NBD and 220 mL dimethyl benzene)

The QC formation rates over per gram total catalyst and per gram titanium were calculated to evaluate the productivity of materials, as shown in Table 2. From the point view of application, MCM-41(30) is most suitable for QC production due to its highest productivity. Regarding to the activity of different Ti species, however, the order is as follows: Ti–MCM-41(70) > Ti–MCM-41(50) > Ti–MCM-41(30) > TiO_2–MCM-41 > TiO_2. Catalyst characterizations have shown that most of the Ti species are incorporated in the framework of Ti–MCM-41(70), but some non-framework Ti and even polymerized species appear with increasing Ti content. In the case of TiO_2–MCM-41, Ti ions predominantly exist in polymerized species. It can be seen that the framework Ti species are most active, and the polymerized species follows. As an extreme, bulk TiO_2 has the lowest activity.

3.7 Possible Reaction Mechanism

The classical triplet state isomerization mechanism used for sensitizer-catalytic reaction is not suitable to explain the present result, because the vertical triplet energy transfer from Ti-oxide species to NBD is very difficult. To facilitate the reaction, NBD molecules should be firstly positively charged by the photoformed holes. However, the free radical ion isomerization mechanism is ruled out because the energy of free $NBD^{\bullet+}$ is significantly lower than free $QC^{\bullet+}$. In fact, the transformation of QC to NBD is through the $QC^{\bullet+} \rightarrow NBD^{\bullet+}$ free radical route [24]. Therefore, a reaction mechanism through the charge-transfer intermediate is more suitable. In this process, NBD molecules are adsorbed on the photoexcited Ti-oxide species (Eqs. 1 and 2). Simultaneously, the photoformed holes are transferred to the absorbed molecules (Eq. 3) to form positively NBD species. Then the positively charged species isomerizes to QC species (Eq. 4). Finally QC is released into the liquid phase and the charge is recombined through back electron transfer (Eq. 5).

Table 2 QC formation rate over as-prepared Ti-containing materials

Samples	TiO_2	TiO_2–MCM-41	Ti–MCM-41(30)	Ti–MCM-41(50)	Ti–MCM-41(70)
Based on total catalyst (mmol h^{-1} g_{catal})	40.8	65.9	71.1	67.5	62.6
Based on TiO_2 (mmol h^{-1} g_{TiO2})	40.8	680.9	5400.2	7448.2	8605.8

Note QC formation rate is an average of 12-h reaction

$$TiO_2 \xrightarrow{h\nu} TiO_2^{\delta-\cdots\delta+} \quad (1)$$

$$TiO_2^{\delta+\cdots\delta-} + NBD \rightarrow TiO_2^{\delta+\cdots\delta-} \cdots NBD \quad (2)$$

$$TiO_2^{\delta+\cdots\delta-} \cdots NBD \rightarrow TiO_2^{-} \cdots NBD^{+} \quad (3)$$

$$TiO_2^{-} \cdots NBD^{+} \rightarrow TiO_2^{-} \cdots QC^{+} \quad (4)$$

$$TiO_2^{-} \cdots QC^{+} \rightarrow TiO_2 + QC \quad (5)$$

4 Conclusions

Ti-containing MCM-41 materials have been synthesized for the photocatalytic isomerization of NBD to QC. Chemical grafting generates TiO_2 crystallites highly dispersed in the pore of MCM-41, which does not influence the textural structure of parent materials. Isomorphous substitution results in the incorporation of Ti into the framework, which significantly interrupts the ordered pore structure of MCM-41, but some nonframework Ti species are formed with increasing Ti content. For the photocatalytic reaction, the yield of QC is Ti–MCM-41(30) > Ti–MCM-41(50) > TiO_2–MCM-41 > Ti–MCM-41(70) > TiO_2. Meanwhile the isolated framework Ti species are most active, the polymerized species follows, and the bulk oxide shows the lowest activity.

Acknowledgments The support from fundamental research project of COSTIND (A1420060192) is greatly appreciated.

References

1. Marzio R, Antonio S, Federico F, Carlo F (1999) Inorg Chem 38:1520
2. Dubonosov AD, Bren VA, Chernoivnov VA (2002) Russian Chem Rev 71:917
3. Kassaee MZ, Vessally E (2005) J Mol Struct Theochem 716:159
4. Bai SD, Dumbacher P, Cole JW (2002) NASA/TP-2002-211729
5. Nichols R, Mckelvey TA, Rodgers SL (1997) US 5616882
6. Schneider SJ (2001) US 6311477
7. Akioka T, Inoue Y, Yanagawa A, Hiyamizu M, Takagi Y, Sugimori A (2003) J Mol Catal A: Chem 202:31
8. Cuppoletti A, Dinnocenzo JP, Goodman JL, Gould IR (1999) J Phys Chem A 103:11253
9. Petrov VA, Vasil'ev NV (2006) Curr Org Synth 3:215
10. Lahiry S, Haldar C (1986) Solar Energy 37:71
11. Ghandi M, Rahimi A, Mashayekhi G (2006) J Photochem Photobiol A: Chem 181:56
12. Hoffmann MR, Martin ST, Choi W, Bahnemann DW (1995) Chem Rev 95:69
13. Hu Y, Higashimoto S, Martra G, Zhang J, Matsuoka M, Coluccia S, Anpo M (2003) Catal Lett 90:161
14. Anpo M, Yamashita H, Ikeue K, Fujii Y, Zhang SG, Ichihashi Y, Park DR, Suzuki Y, Koyano K, Tatsumi T (1998) Catal Today 44:327
15. Hu Y, Martra G, Zhang J, Higashimoto S, Coluccia S, Anpo M (2006) J Phys Chem B 110:1680
16. Do Y-J, Kim J-H, Park J-H, Park S-S, Hong S-S, Suh C-S, Lee G-D (2005) Catal Today 101:299
17. Wang X, Lian W, Fu X, Basset J-M, Lefebvre F (2006) J Catal 238:13
18. Wang X, Xu H, Fu X, Liu P, Lefebvre F, Basset J-M (2005) J Mol Catal A: Chem 238:185
19. Yuan Q, Hagen A, Roessner F (2006) Appl Catal A: Gen 303:81
20. Eimer GA, Casuscelli SG, Ghione GE, Crivello ME, Herrero ER (2006) Appl Catal A: Gen 298:232
21. Galacho C, Ribeiro Carrott MML, Carrott PJM (2007) Microporous Mesoporous Mater 100:312
22. Guo D-S, Ma Z-F, Jiang Q-Z, Xu H-H, Ma Z-F, Ye W-D (2006) Catal Lett 107:155
23. Luo Y, Lu GZ, Guo YL, Wang YS (2002) Catal Commun 3:129
24. Ikezawa H, Kutal C (1987) J Org Chem 52:3299